



## Relationship between gadolinium-based MRI contrast agent consumption and anthropogenic gadolinium in the influent of a wastewater treatment plant



Attila Laczovics<sup>a,b</sup>, István Csige<sup>c</sup>, Sándor Szabó<sup>d</sup>, Albert Tóth<sup>c</sup>, Ferenc Krisztián Kálmán<sup>e</sup>, Imre Tóth<sup>f</sup>, Zoltán Fülöp<sup>g</sup>, Ervin Berényi<sup>a,b</sup>, Mihály Braun<sup>c,\*</sup>

<sup>a</sup> Department of Medical Imaging, Division of Radiology and Imaging Science, Faculty of Medicine, University of Debrecen, H-4032 Debrecen, Nagyterdei krt 98, Hungary

<sup>b</sup> Doctoral School of Neuroscience, Faculty of Medicine, University of Debrecen, H-4032 Debrecen, Nagyterdei krt 98, Hungary

<sup>c</sup> Isotope Climatology and Environmental Research Centre, Institute for Nuclear Research, Hungarian Academy of Sciences, H-4026 Debrecen, Bem tér 18/C, Hungary

<sup>d</sup> Department of Biology, University of Nyíregyháza, H-4401 Nyíregyháza, PO Box 166, Hungary

<sup>e</sup> Department of Physical Chemistry, University of Debrecen, H-4032 Debrecen, Egyetem tér 1, Hungary

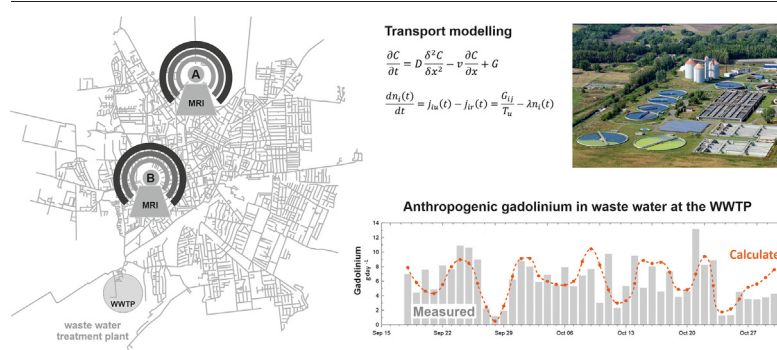
<sup>f</sup> Department of Inorganic and Analytical Chemistry, University of Debrecen, H-4032 Debrecen, Egyetem tér 1, Hungary

<sup>g</sup> Debrecen Waterworks Ltd., H-4025 Debrecen, Hatvan u. 12-14, Hungary

### HIGHLIGHTS

- Release of Gd from patients to sewage system was quantitatively described.
- Overall, 37 % of the administered Gd was recovered at the WWTP.
- Advection-dispersion model was fitted for temporal distribution of Gd in wastewater.
- The speed of Gd release from patient to WWTP was slower than expected.

### GRAPHICAL ABSTRACT



### ARTICLE INFO

Editor: Paola Verlicchi

#### Keywords:

Gadolinium-based contrast agent  
Wastewater treatment  
Advection-dispersion transport model  
Anthropogenic gadolinium  
Inductively coupled plasma mass spectrometry

### ABSTRACT

Gadolinium-based contrast agents (GBCAs) used in magnetic resonance imaging (MRI) are highly resistant in the environment. They pass through wastewater treatment plants (WWTPs) unhindered escaping degradation. Although GBCAs are subjects of intensive research, we recognized that a quantitative approach to the mass balance of gadolinium, based on known input and output data, is missing. The administered amount of Gd as GBCAs, the number of out- and inpatients and the concentration of rare earth elements (REEs) in wastewater were monitored for 45 days in a medium sized city (ca. 203,000 inhabitants) with two MRI centres. An advection-dispersion type model was established to describe the transport of Gd in the wastewater system. The model calculates with patient locality, excretion kinetics of Gd and the yield of wastewater. The estimated and measured daily amount of anthropogenic gadolinium released to the WWTP were compared. GBCAs (Omniscan and Dotarem) were administered to 1008 patients representing a total of  $700 \pm 1$  g Gd. The amount of total Gd entering the WWTP was  $531 \pm 2$  g, of which the anthropogenic contribution (i.e. GBCAs) was  $261 \pm 6$  g ( $49 \pm 1$  % of the total Gd) during the sampling campaign. Local residents and inpatients should fully release Gd in the city, but outpatients only partially. Overall,  $37 \pm 1$  % of the total administered

\* Corresponding author.

E-mail address: [braun.mihaly@atomki.hu](mailto:braun.mihaly@atomki.hu) (M. Braun).

Gd was recovered in the wastewater, so the remaining  $63 \pm 1\%$  of administered Gd is expected to be dispensed outside of the sewer system. Our approach enables to better understand the dispersion of GBCAs originated Gd in an urban environment.

## 1. Introduction

Gadolinium-based contrast agents (GBCAs) have become one of the most successful metal-containing drugs over at least the last three decades. The success of GBCAs can be attributed to the high value of diagnostic information and safety statistics compared with other diagnostic agents (Wahsner et al., 2019). As the number of patients has exceeded 30 million per year, the consumption of GBCAs has increased drastically during the last few decades (Lohrke et al., 2016). Up to 2018, over 450 million GBCA doses have been administered globally (McDonald et al., 2018; Tircsó et al., 2021). Estimating 1 g Gd(III) per dose the cumulative mass of gadolinium can be calculated to be 4500 tons, which has been mobilized in GBCAs and drained into the wastewater systems (Brünjes and Hofmann, 2020). The contribution of industry (e.g. magnetic bubble memory devices, optical fibres and optical discs in magneto-optical recording technology) to the release of gadolinium could also be significant (Deboer and Lammertsma, 2013; Du and Graedel, 2011; Gonzalez et al., 2014; Hayes-Labruto et al., 2013). However, they are globally less widespread and they located to well defined regions.

GBCAs can be classified depending on their chemical structure and charge. Omniscan (Gd-DTPA-BMA), which is a non-ionic linear type, and Dotarem (Gd-DOTA), which is an ionic macrocyclic type were used in this study. They are administered intravenously to patients with a normal dose of  $0.1 \text{ mmol} \cdot \text{kg}^{-1}$ . Within 24 to 48 h through urination after the total amount of GBCAs administered to patients enters the regional wastewater system (Swan et al., 1999). Direct appearance of Gd in the wastewater originated from MRI centres has been reported (Bau and Dulski, 1996; Kulaksız and Bau, 2007; Rabiet et al., 2009; Telgmann et al., 2012).

Several studies have suggested that GBCAs are likely to be resistant to degradation (Lawrence et al., 2009; Holzbecher et al., 2005; Verplanck et al., 2005). Neither wastewater treatment plants (WWTPs) (Möller et al., 2002; Verplanck et al., 2010; Ebrahimi and Barbieri, 2019), nor aquatic plants (Braun et al., 2018; Kartamihardja et al., 2022) are able to considerably reduce the amount of anthropogenic Gd related to GBCAs in the water. However, Birka et al. (2016) pointed out degradation of various GBCAs by UV radiation in drinking and surface waters. A novel field survey (Zocher et al., 2022) has also pointed out that anthropogenic Gd as GBCA-s are not accumulated in free-floating plant species (e.g. duckweeds). Therefore, considerable proportion of Gd passes through the WWTPs and finally reaches continental surface waters (Bau and Dulski, 1996; Zhu et al., 2004; de Campos and Enzweiler, 2016), seas and oceans (Hatje et al., 2016, 2018; Kulaksız and Bau, 2007). It was also reported that in marine environment free ionic Gd can be effectively accumulated by macroalgae (Ferreira et al., 2020; Kartamihardja et al., 2022) and that it can have toxic effect in mussels (Henriques et al., 2019).

The high stability of these gadolinium-containing compounds enables them to penetrate through riverbank filtration wells and even through drinking water treatment plants (Holzbecher et al., 2005; Schmidt et al., 2019). Abnormally high gadolinium levels are reported in the drinking water of some large cities (Kulaksız and Bau, 2011). Although no severe adverse biological effect has been reported so far, the emerging environmental concern is obvious (Ebrahimi and Barbieri, 2019). Human oral uptake of GBCAs from drinking water has to be considered, since gastric fluid decomposes GBCA-s allowing Gd to enter the blood stream (Souza et al., 2021).

Several studies have been published on monitoring the concentration of Gd in the effluent of hospitals, in wastewaters as well as in the outflow of WWTPs (Künnemeyer et al., 2009; Lawrence et al., 2009). Speciation analysis of Gd was performed by Künnemeyer et al. (2009) in hospital

effluents. They pointed out using HILIC/ICP-MS that almost 100 % of the total Gd was in form of various GBCAs.

Despite of excessive study of GBCAs, research addressing the overall mass balance of GBCAs from MRI centres to WWTPs is missing. The aim of this study to fill this gap completely. Thus, we investigated the daily consumption of GBCAs for a 45-day period in a medium-sized city (c.a. 203,000 inhabitants) with two MRI centres. Gd has no other anthropogenic source in this city. The wastewater treatment plant (WWTP) provided daily average water samples and wastewater flow data for the period of interest. The concentration of Gd was measured, and the daily amount of anthropogenic Gd entering the WWTP with the raw wastewater has been estimated. An advection-dispersion model was developed to describe the spatial and temporal distribution of Gd released into the wastewater system.

## 2. Materials and methods

### 2.1. MRI centres

Our investigation was conducted in Debrecen, which is a medium-sized city in eastern Hungary with c.a. 200,000 inhabitants. There are two MRI centres (Fig. 1. A and B) which serve patients mainly the north-eastern region of the country, as well as from abroad. Both facilities are situated in the Clinical Centre, University of Debrecen. The centres used Omniscan and Dotarem for contrast enhancement. The total number of patients was 6731 and the amount of administered Gd was 4500 g in the year of the study in 2014. The MRI centres provided all data of administered GBCA doses together with the postcode of residence for each patient.

The time frame of the study was 45 days (from 17th of September until 31st of October). During this period, the total number of contrast enhanced examinations was 1008. The total amount of administered Gd was  $700 \pm 1 \text{ g}$ . Uncertainty of GBCA administration was calculated by considering the prescription of ISO 7886-1:1993, which was in force at time of the investigations. We calculated with 4 % of relative error of the volume was given to the patients, and error propagation was used for calculating the daily amount of the administered Gd. There was still some GBCA left in the vials, but these were collected separately and did not get to wastewater pipe as anthropogenic Gd. The daily amount of Gd administered to the patients are given in Table A.1. in the online supplementary material.

### 2.2. Wastewater system

The WWTP of Debrecen utilizes biological wastewater treatment with an activated sludge process. The total length of the wastewater drainage system is 612 km in Debrecen (Fig. 1), the distance between the farthest point and the WWTP is about 10 km. The daily amount of wastewater varies between 30,000 and 50,000  $\text{m}^3$ , depending on seasonal changes in water consumption and weather conditions (Table A.2. in the online supplementary material). The wastewater yield at the WWTP shows a regular daily variation with reduced yield between 2 and 7 am by about a factor of two compared with average daylight yield. The volume of the daily amount of wastewater was measured using an electromagnetic flowmeter (produced by Endres & Hauser). The guaranteed relative error of volume measurement was  $\pm 0.5\%$  (provided by the company). It was an accredited measurement of the WWTP. The flow velocity of wastewater was around 0.7 m/s. The residence time of wastewater in the drainage system was less than 1 day (typically 4–8 h).

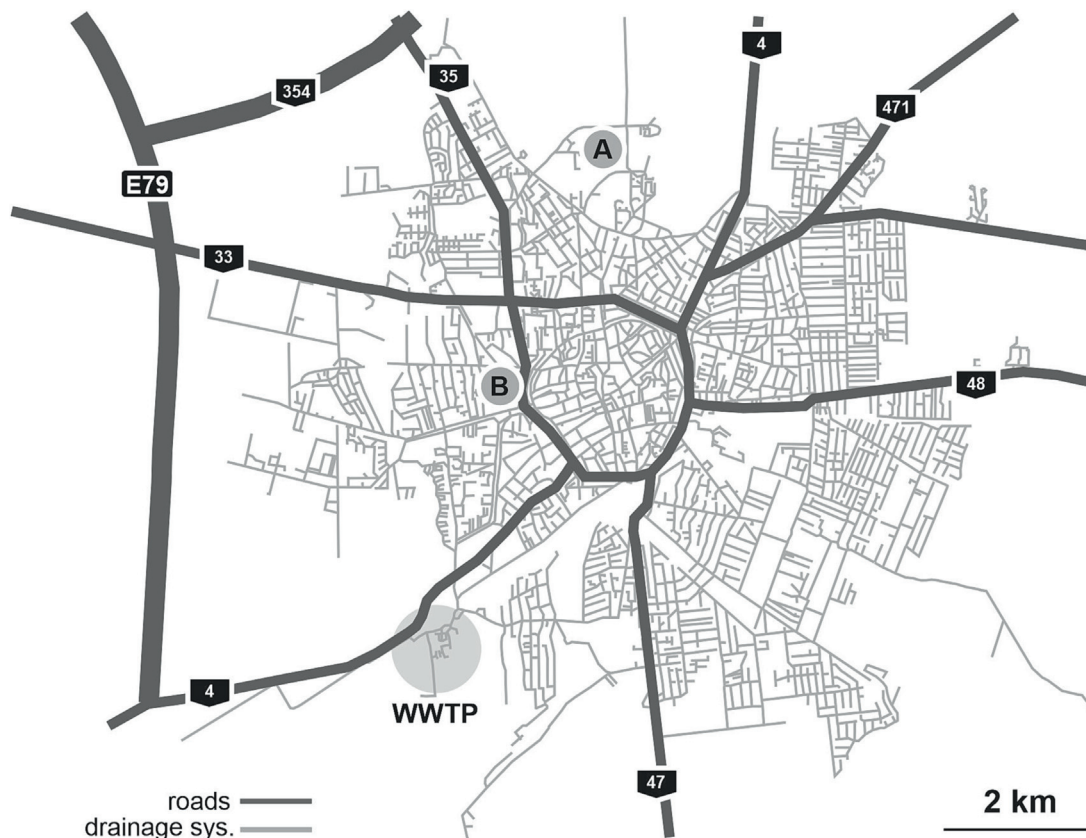


Fig. 1. The MRI centres (A and B), the wastewater treatment plant (WWTP) and the drainage system in Debrecen.

### 2.3. Wastewater sampling and analytical procedure

Fixed volume composite samples (representing a 24-h average) were taken from the raw wastewater using an automated sampler (with 1 h sampling frequency) at the inlet to the WWTP. Sampling was started at 8:00 a.m. on September 17 and finished at 8:00 a.m. on October 31, 2014. Each daily sampling run started at 8:00 a.m. and ended at 8:00 on the next day. The latter was considered as the sampling date. This way of sampling did not represent the effect of daily variation in the wastewater yield, since the flow rate of wastewater decreased to half of the daily rate during night. As a result, the averaged samples were overrepresented in the period between 2:00 and 7:00 a.m. by a factor of two.

During the sample pretreatment, 25 mL of homogenized wastewater samples were dispensed into teflon bombs. Organic substances were decomposed with 3 mL of 67 % (m/m) nitric acid and 2 mL of 37 % (m/m) hydrochloric acid. All reagents were suprapure grade produced by Molarchem. The samples were processed using a Mars 5 microwave system at 165 °C for 30 min. Blank samples were also prepared for each batch with the same method. The concentration of rare earth elements (REEs) were determined using an Agilent 8800 inductively coupled plasma mass spectrometer (ICP-MS). Three parallel measurements of the digested samples were made by ICP-MS for rare earth elements. The parameters (Table A.3) and detection limits (Table A.4), which were determined by measuring 10 replicates of blank samples, and the concentrations of rare earth elements (Table A.5) are in the online supplementary material.

### 2.4. Calculation of the Gd anomaly and anthropogenic Gd flux

Rare earth element data were normalized to Post Archean Australian Shale (PAAS) (Nance and Taylor, 1976). Plotting the normalized concentrations against the atomic numbers for anthropogenically unaffected samples, the shale normalized patterns are usually smooth. The shale normalized

concentration of any lanthanides ( $Ln_{SN}^*$ ) can be predicted by linear extrapolation or polynomial modelling of the shape of the REE pattern (Lawrence et al., 2009). Actually, we applied third order polynomial regression using normalized concentrations of Nd, Sm, Dy, Ho, Er, Tm and Yb for estimating the concentration of natural gadolinium ( $Gd_{SN}^*$ ) and europium ( $Eu_{SN}^*$ ). The variance of the background (geogenic) concentration was obtained from the error of the fitting. High concentrations of normalized values were found for La and Ce in the wastewater samples, therefore these elements were excluded from the calculations (Kulaksız and Bau, 2007). Pr and Lu were also excluded from the calculations owing to their low concentration. Terbium was excluded, because it was used as internal standard.

The natural background pattern of REE is fitted by polynomial function as shown in Fig. 2. A europium anomaly has not been found in our case. Therefore this element was used for the verification of the normalization procedure (Fig. 2). The measured ( $Eu_{SN}$ ) and the calculated ( $Eu_{SN}^*$ ) normalized values showed a strong correlation ( $r = 0.992$ ).

The Gd anomaly had been defined by the ratio  $Gd_{SN}/Gd_{SN}^*$ , where the numerator was the normalized value of the measured Gd and the denominator was the calculated natural background. Positive Gd anomaly was defined by ratios larger than 1.1.

Anthropogenic gadolinium ( $Gd_{ant}$ ) is usually estimated using Eq. (1):

$$Gd_{ant} = (Gd_{SN} - 1.1 \cdot Gd_{SN}^*) \cdot Gd_{PAAS} \quad (1)$$

where  $Gd_{SN}$  is the normalized value of the measured Gd,  $Gd_{SN}^*$  is the normalized value of the estimated natural Gd (geogenic background), and  $Gd_{PAAS}$  is the concentration of Gd in the reference shale (PAAS). The factor of 1.1 is an empirically defined parameter (Lawrence et al., 2009). The daily amount of total and anthropogenic Gd are calculated by multiplying the daily average Gd concentration by the daily volume of wastewater. Since the estimated Eu backgrounds showed a good correlation with the measured values, we assumed that the estimation of the Gd background

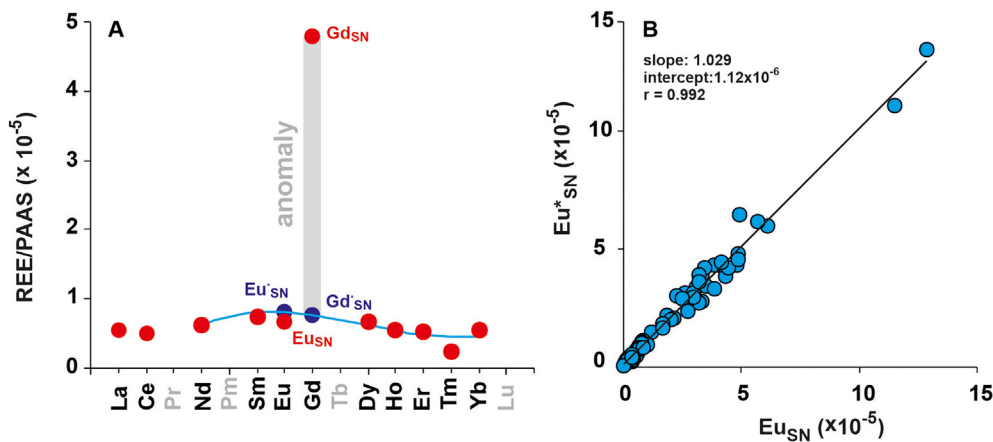


Fig. 2. PAAS normalized rare earth elements pattern with fitted background (A), and comparison of measured and estimated backgrounds of europium (B).

was also adequate. Therefore, we calculate the anthropogenic Gd using Eq. (2).

$$Gd_{ant}^* = (Gd_{SN} - Gd_{SN}^*) \cdot Gd_{PAAS} \quad (2)$$

Anthropogenic anomaly of Gd was found for each sampling day, the minimum of  $Gd_{SN}/Gd_{SN}^*$  was 1.3, while the maximum was 6.5. The average anomaly of the sampling campaign was  $2.4 \pm 1.2$ . The anthropogenic Gd fraction was significantly higher than the geogenic, thus it can be used as an estimate for the contribution of GBCAs. The total amount of anthropogenic Gd was  $261 \pm 6$  g during the investigated time period. There is no other e.g. industrial source of Gd in Debrecen, hence we can assume that all the anthropogenic Gd can be attributed to GBCAs. Concentrations of geogenic ( $Gd_{geo}$ ) and anthropogenic gadolinium ( $Gd_{ant}$ ) are given in Table A.5. in the online supplementary material. Daily amounts of total, geogenic and anthropogenic Gd are given in Table A.6. in the online supplementary material.

#### 2.4.1. Uncertainty of the results

To evaluate the uncertainty of the results an error propagation package of Python (<https://pythonhosted.org/uncertainties/>) was used. We had the variances of the measurements of the total Gd concentrations based on the three parallel measurements of the samples. The geogenic background Gd concentration was estimated using 3rd order polynomial regression, using the concentration of Nd, Sm, Dy, Ho, Er, Tm and Yb. The variances of the background concentrations were obtained from the error of the fitting. The error of the anthropogenic Gd was calculated using error propagation that combines the variances for the differences of the total Gd and the geogenic background of the Gd. The guaranteed relative error was  $\pm 0.5$  % for the volume of wastewater. For uncertainty of GBCA administration, we calculated with 4 % (ISO 7886-1:1993) of relative error. The total amounts and their uncertainties are given in Table A.7. in the online supplementary material.

## 2.5. Transport modelling

### 2.5.1. Governing equation

The sewerage system (Fig. 1) shows a complex network of channels. The flow direction of wastewater is always the same at any point in the channels. Therefore, it is possible to sum up the water yields of those parts of the channel system from which wastewater makes the same distance to reach the WWTP. For this reason, we have substituted the network with a single, one-dimensional channel with a length of  $L$ , which is the length between the most distant entry point of the network and the WWTP.

Anthropogenic gadolinium ( $Gd_{ant}$ ) was estimated representing the Gd of GBCAs in wastewater in this study. We assumed that the interaction with solid particles is negligible. Therefore,  $Gd_{ant}$  is considered as a

conservative solute in wastewater which is not adsorbed by solid walls or sediments in the channel (Elizalde-González et al., 2017; Künnemeyer et al., 2009). The transport of such a solute then may be described by the one-dimensional advection-dispersion Eq. (3) (El Kadi Abderrezzak et al., 2015).

$$\frac{\partial C}{\partial t} = D \frac{\delta^2 C}{\delta x^2} - v \frac{\partial C}{\partial x} + G \quad (3)$$

where:  $C(x, t)$ : the concentration of the solute ( $Gd_{ant}$ ) in wastewater ( $\text{mol m}^{-3}$ );  $D$ : longitudinal dispersion coefficient, in the order of  $10\text{--}100 \text{ m}^2 \text{ s}^{-1}$  (El Kadi Abderrezzak et al., 2015; Zeng and Huai, 2014);  $v$ : average transport velocity of  $Gd_{ant}$  in the sewage channels ( $\text{m s}^{-1}$ );  $G(x, t)$ : source term (the amount by which the  $Gd_{ant}$  concentration increases at a given location and at a given time as a result of Gd excretion by patients) ( $\text{mol m}^{-3} \text{ s}^{-1}$ ).

The above partial differential equation was solved using the finite differences method. In terms of modelling the transport of pollutant, no diffusion-flow boundary condition was applied to the boundaries of the domain. As the initial condition, we began with GBCA-free wastewater.

### 2.5.2. Release scenario

The release of Gd to the sewerage network shows complex spatial and temporal variations. The process starts with the uptake of Gd by the patients at the two MRI Centres (MRI-A and MRI-B, Fig. 1) followed by gradual release of gadolinium by the patients partly in the MRI centres, partly distributed over the sewerage network and partly outside the network system. Therefore, we have defined three types of sources: (1) *Gd-release at the MRI-A*, (2) *Gd-release at the MRI-B*, (3) *Gd-release distributed evenly over the sewerage network of the city*.

The patients were divided into six groups: ( $G_1$ ) *MRI-A inpatients*, ( $G_2$ ) *MRI-A outpatients from Debrecen*, ( $G_3$ ) *MRI-A outpatients not from Debrecen*, ( $G_4$ ) *MRI-B inpatients*, ( $G_5$ ) *MRI-B outpatients from Debrecen*, ( $G_6$ ) *MRI-B outpatients not from Debrecen*.

The schedule of MRI scanning and the amount of administrated Gd to each patient has been recorded. The dosage and pharmacokinetic properties of Dotarem and Omniscan are similar, therefore we can handle them together in the model calculations. We have calculated the daily amount of Gd uptake for each group ( $G_{ij}$ ), by summing up the individual doses administered to patients, where  $i = 1 \dots 6$  is the number of the group and  $j = 1, \dots, 45$  is the number of the day.

We have assumed that the daily Gd uptake is evenly distributed between 7:00 a.m. and 09:00 p.m. and that the rate of excretion is always proportional to the amount of Gd present in patients at a time. The elimination constant ( $\lambda = \ln(2)/T_{1/2}$ ) is calculated from the biological elimination half-life ( $T_{1/2} = 1.7\text{h}$ ) of Gd in the patients (Aime and Caravan, 2009).

The rate of change of the amount of Gd, that can be found in the bodies of patients of a given (*i*) group can be described by the differential Eq. (4).

$$\frac{dn_i(t)}{dt} = j_{iu}(t) - j_{ir}(t) = \frac{G_{ij}}{T_u} - \lambda n_i(t) \quad (4)$$

where,  $n_i(t)$ : the amount of Gd in the patients of the group *i*, mol;  $j_{iu}(t) = G_{ij}/T_u$ : Gd uptake rate, mol s<sup>-1</sup>;  $j_{ir}(t) = \lambda n_i(t)$ : Gd elimination rate, mol s<sup>-1</sup>;  $T_u = 50400$ s: Gd uptake period.

The solution of the above differential equation in the period between 7:00 a.m. – 9:00 p.m. is  $n_i(t) = n_i(1 - e^{-\lambda t})$  and for the period between 9:00 p.m. - 7:00 a.m. the next day  $n_i(t) = n_{i21}e^{-\lambda t}$ , where  $n_i = G_{ij}/(\lambda T_u)$  and  $n_{i21} = n_i(1 - e^{-\lambda T_u})$  is the total amount of Gd in the patients at 9:00 p.m.

It has been assumed that all inpatients release the total amount of Gd at the sites of the MRI centres. Furthermore, we have assumed that all (including local and non-local) outpatients also eliminate some of the Gd at the MRI centres, where the GBCA was administered to them. This is achieved by assuming that following GBCA administration all outpatients spend the same period of time ( $T_h$ ) at the MRI centres. After this period, we have assumed all local and part of the non-local ( $R_{nl}$ ) outpatients eliminate

Gd distributed evenly over the whole sewage system of the city. Finally, following this period, only local outpatients released Gd in the city.

### 2.5.3. Parameter estimation

There are several parameters in the transport model that must be estimated. We used trial and error method to find the values of the following parameters:  $\nu, T_h \wedge R_{nl}$ . For parameter estimation, we used the Root-Mean-Square of Normalized Differences (RMSND),

$$RMSND = \sqrt{\frac{\sum_{i=1}^n \left( \frac{m_i^m - m_i^c}{m_i^m} \right)^2}{n}}$$

where  $m^m$  is the measured and  $m^c$  is the calculated daily amount of anthropogenic gadolinium ( $G_{am}$ ) released to the WWTP, and  $n$  is the number of days ( $n = 45$  days). Calculations were performed using our own custom-developed software.

## 3. Results and discussion

Daily amounts of Gd administered to inpatients ( $G_1, G_4$ ), local ( $G_2, G_5$ ) and non-local ( $G_3, G_6$ ) outpatients are presented in Fig. 3. The daily amount

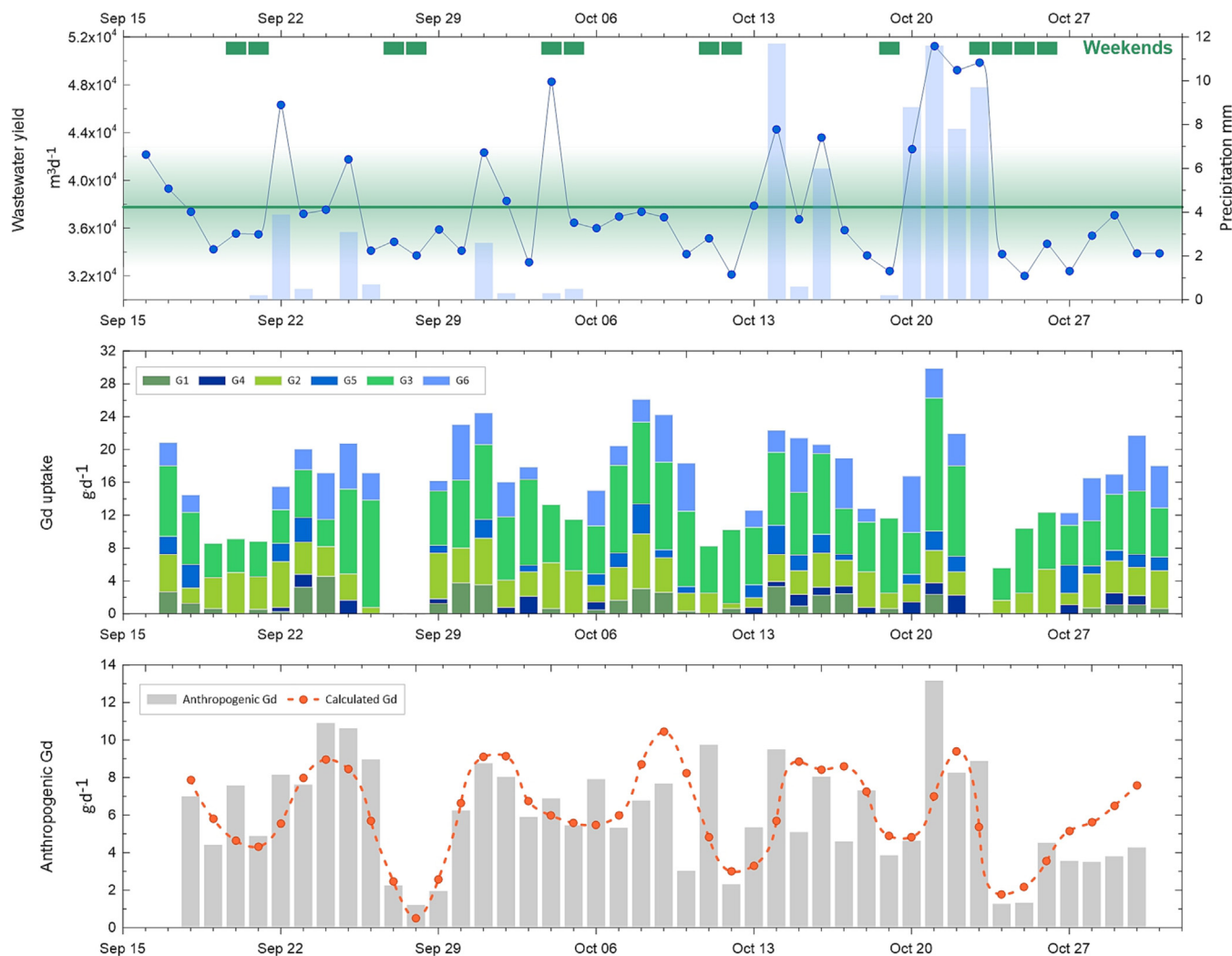


Fig. 3. Upper panel: wastewater yield (blue dots), precipitation (pale blue bars). Weekends and national holidays are marked with dark green boxes. Middle panel: daily amount of Gd (uptake) administered to the different groups ( $G_1$ ) MRI-A inpatients, ( $G_2$ ) MRI-A outpatients from Debrecen, ( $G_3$ ) MRI-A outpatients not from Debrecen, ( $G_4$ ) MRI-B inpatients, ( $G_5$ ) MRI-B outpatients from Debrecen, ( $G_6$ ) MRI-B outpatients not from Debrecen of patients. Lower panel: measured (gray) and calculated (red) amount of anthropogenic gadolinium.

of administered Gd is highly variable depending on the activity of MRI centers (e.g. drops occur on weekends or on national holidays).

Total concentrations of Gd ( $G_{tot}$ ) in the primary influent wastewater samples ranged from 60 to 845  $\text{ng L}^{-1}$ , mean  $321 \pm 150$  (SD)  $\text{ng L}^{-1}$  that is an elevated level compared to the range c.a. 30–300  $\text{ng L}^{-1}$  reported for wastewaters in the U.S.A., Germany and Australia (Ebrahimi and Barbieri, 2019; Lawrence et al., 2009; Telgmann et al., 2012; Verplanck et al., 2010;). The total inflow volume of wastewater was 1,621,436  $\text{m}^3$  in the investigated period. Fluctuations in wastewater volume were small, while the daily amount of  $G_{tot}$  showed more dynamic variations without apparent periodicity (Fig. 3.). The total amount of Gd, calculated from the measured Gd concentrations and daily wastewater yields, was  $531 \pm 2$  g for the investigated period. The anthropogenic fraction of Gd was  $261 \pm 6$  g ( $49 \pm 1$  %) and the geogenic fraction was  $272 \pm 6$  g ( $51 \pm 1$  %) of the total. Nearly the half of Debrecen city is situated in a loess covered area. Significant prevalence of geogenic fraction of Gd can be explained by the richness of REEs in loess (Qizhong et al., 1985). Since no other industrial source of Gd exists, we can assume that  $G_{d_{ant}}$  represents the GBCA related Gd. In fact  $37 \pm 1$  % of Gd administered to the patients was recovered in the wastewater.

Amount of Gd administered to the inpatients ( $G_1$ ,  $G_4$ ) and local outpatients ( $G_2$ ,  $G_3$ ) was (264 g, 38 %). It is in unexpectedly good agreement with the recovered amount of  $G_{d_{ant}}$  ( $261 \pm 6$  g). The two MRI centres and more than 95 % of the households in Debrecen are connected to the sewage system. In spite of this, we cannot exclude of Gd retention or loss in the sewage system. However, it has to be considered that patients non-Debrecen residents received 436 g of Gd (62 %), and they also may have a substantial contribution to the Gd in the sewage system. Patients spend some time at the MRI centres, where many of them are likely to pass urine in the hospital shortly after the MRI investigation. Furthermore, following the CE-MRI examination, a fraction ( $R_{nl}$ ) of these non-local outpatients spend hours in the city (restaurant, shopping, etc.). During this period they may also excrete Gd mostly in the central part of the city. The contribution of non-local patients, who usually do not stay in the city overnight, cannot be determined directly.

We optimized the parameters of the model by minimizing the RMSND using the trial and error method. Daily amounts of Gd in wastewater estimated by the model are given in Table A.6. in the online supplementary material. A correlation plot of the measured and estimated daily amounts of anthropogenic Gd is given in Fig. 4.

A minimum RMSND was found when we assumed that outpatients stayed in the hospitals for 15 min following the CE-MRI examination, 10 % of non-local outpatients stayed the whole day in the city. The



Fig. 4. Scatterplot of the measured and calculated daily amount of anthropogenic gadolinium released to the wastewater treatment plant.

behaviour of patients was not observed during this pilot study. However, this habit of patients agreed with the experience of healthcare professionals of these MRI centres (personal communication).

In the best-fit model, the parameter of transport velocity of anthropogenic Gd (0.080 m/s) was out of the range of the velocity of wastewater required by sewer design. The optimum velocity of wastewater flow is 0.7 m/s, and technically allowed minimum is 0.4 m/s. It may imply that the anthropogenic Gd migrates slower than the water in the channel.

Examinations are not performed on weekends or national holidays in the MRI centres. In our time frame there were two occasions when no patients were examined and the input of Gd to the sewage system was zero. Cross correlation analysis revealed periodicity, which followed a weekly working activity. Similar pattern was reported by Telgmann et al. (2012) for the city of Münster in a sampling campaign carried out in autumn. The time lag in the pattern of the anthropogenic Gd in wastewater relative to the administered Gd could be maximum 1 day owing to the excretion kinetics of Gd and the velocity of the water flow in the sewer network. In spite of this, the time lag in Debrecen was found to be 2 days (Fig. A.1. in the online supplementary material) which needs further discussion.

The simplest answer would be if we supposed a longer residence time of wastewater in the sewage system. The length of the sewer channels and the velocity of the water flow are parameters well defined by the Waterworks Ltd. in Debrecen. The design of the canalisation assures that the maximum residence time is less than 24 h. Therefore, this explanation cannot be accepted.

GBCAs are highly resistant and well soluble in water, hence they should be transported by the water phase. A lower transport rate may be explained if the anthropogenic Gd is bound to particulate matter, which moves slower than the water and water dissolved materials. In this study we analysed unfiltered wastewater samples after digestion. The water soluble and the particle matter bound Gd (if any) was not differentiated. Further speciation analysis of Gd and GBCAs would be necessary to clarify the observed unexpected behaviour of Gd in the sewage system.

We also may consider the possibility the lower rate of GBCA excretion from the human body. Pharmacokinetic properties of GBCAs are well investigated, and the half life values (used also in our model) are well established (Baranyai et al., 2015). However, there are studies which reported longer (3 days to month) excretion pattern of GBCAs in urine (Grimm and Williams, 2018). We also have to consider the behaviour and health status of a larger population. A lower but still normal renal function may elongate the elimination of GBCAs. Patients are encouraged to drink large amount of water after an MRI examination, what they might disregard, which also leads to slower excretion. We believe that the urination habit of patients may be the most likely background factor behind the observed phenomena. The bladder could be considered as a temporary collecting pool of GBCAs, which could prolong the output of Gd. Timing of urination (first occasion after MRI, number of times per day) and volume of urine may have a complex effect. Higher temporal resolution of wastewater sampling (e.g. 2 h for a week) may be suitable to clarify the observed time lag combining with a simultaneous logging of GBCA consumption.

#### 4. Conclusion

We proposed a quantitative model to describe the relationship between the daily consumption of GBCAs in MRI centres and the observed amount of anthropogenic Gd in wastewater. Result of model calculation draws attention to the transport of Gd from the human body through the sewage system. A two-day time lag was found between the temporal pattern of administered GBCAs and the anthropogenic Gd measured at the inlet to WWTP. The model highlights that this phenomenon cannot be simply explained by hydraulic properties of sewage system. Although the temporal pattern of anthropogenic Gd in the wastewater was described precisely, the slow transport of Gd in the sewage system predicted by the model, needs further investigations. We should consider that release of GBCAs from the human body may take longer under real life circumstances than under optimal clinical condition.

## CRediT authorship contribution statement

Attila Laczovics: Data curation, Investigation, Writing - original draft preparation; István Csige: Methodology, Software, Formal analysis, Visualization; Sándor Szabó: Writing - original draft preparation review & editing; Albert Tóth: Writing - original draft preparation review & editing, Visualization; Ferenc Krisztián Kálmán: Investigation; Imre Tóth: Conceptualization, Writing - review & editing; Zoltán Fülöp: Resources, Data curation; Ervin Berényi: Conceptualization, Supervision, Project administration; Mihály Braun: Conceptualization, Investigation, Visualization, Writing - original draft preparation review & editing, Resources.

## Data availability

Data will be made available on request.

## Declaration of competing interest

The authors declare that they have no known competing financial interests or personal relationships that could have appeared to influence the work reported in this paper.

## Acknowledgements

The research was supported by the European Union and the State of Hungary, co-financed by the European Regional Development Fund in the project of GINOP-2.3.2-15-2016-00009 “ICER”, Hungarian National Research, Development and Innovation Office (NKFIH, K-134694), and by the Scientific Council of the University of Nyíregyháza. We would like to thank Timothy Jull for his comments on the manuscript and for Ádam Braun for the error propagation calculations. The critical comments of the anonymous reviewers helped us to improve the manuscript considerably.

## Appendix A. Supplementary data

Supplementary data to this article can be found online at <https://doi.org/10.1016/j.scitotenv.2023.162844>.

## References

- Aime, S., Caravan, P., 2009. Biodistribution of gadolinium-based contrast agents, including gadolinium deposition. *J. Magn. Reson. Imaging* 30, 1259–1267. <https://doi.org/10.1002/jmri.21969>.
- Baranyai, Z., Brücher, E., Uggeri, F., Maiocchi, A., Tóth, I., András, M., Gáspár, A., Zékány, L., Aime, S., 2015. The role of equilibrium and kinetic properties in the dissociation of Gd [DTPA-bis(methylamide)] (Omniscan) at near to physiological conditions. *Chem. Eur. J.* 21, 4789–4799. <https://doi.org/10.1002/chem.201405967>.
- Bau, M., Dulski, P., 1996. Anthropogenic origin of positive gadolinium anomalies in river waters. *Earth Planet. Sci. Lett.* 143, 245–255. [https://doi.org/10.1016/0012-821X\(96\)00127-6](https://doi.org/10.1016/0012-821X(96)00127-6).
- Birka, M., Roscher, J., Holtkamp, M., Sperling, M., Karst, U., 2016. Investigating the stability of gadolinium-based contrast agents towards UV radiation. *Water Res.* 91, 244–250.
- Braun, M., Zavanyi, G., Laczovics, A., Berényi, E., Szabó, S., 2018. Can aquatic macrophytes be biofilters for gadolinium-based contrasting agents? *Water Res.* 135, 104–111. <https://doi.org/10.1016/j.watres.2017.12.074>.
- Brünjes, R., Hofmann, T., 2020. Anthropogenic gadolinium in freshwater and drinking water systems. *Wat. Res.* 182, 115966.
- de Campos, F.F., Enzweiler, J., 2016. Anthropogenic gadolinium anomalies and rare earth elements in the water of Atibaia River and Anhumas Creek, Southeast Brazil. *Environ. Monit. Assess.*, 188 <https://doi.org/10.1007/s10661-016-5282-7>.
- Deboer, M.A., Lammertsma, K., 2013. Scarcity of rare earth elements. *ChemSusChem* 6, 2045–2055. <https://doi.org/10.1002/cssc.201200794>.
- Du, X., Graedel, T.E., 2011. Global rare earth in-use stocks in NdFeB permanent magnets. *J. Ind. Ecol.* 15, 836–843. <https://doi.org/10.1111/j.1530-9290.2011.00362.x>.
- Ebrahimi, P., Barbieri, M., 2019. Gadolinium as an emerging microcontaminant in water 405 resources: threats and opportunities. *Geosciences* 9, 93. <https://doi.org/10.3390/geosciences9020093>.
- El Kadi Abderrezzak, K., Ata, R., Zaoui, F., 2015. One-dimensional numerical modelling of solute transport in streams: the role of longitudinal dispersion coefficient. *J. Hydrol.* 527, 978–989. <https://doi.org/10.1016/j.jhydrol.2015.05.061>.
- Elizalde-González, M.P., García-Díaz, E., González-Pereira, M., Mattusch, J., 2017. Removal of gadolinium-based contrast agents: adsorption on activated carbon. *Environ. Sci. Pollut. Res.* 24, 8164–8175. <https://doi.org/10.1007/s11356-017-8491-x>.
- Ferreira, N., Ferreira, A., Viana, T., Lopes, C.B., Costa, M., Pinto, J., Soares, J., Pinheiro-Torres, J., Henriques, B., Pereira, E., 2020. Assessment of marine macroalgae potential for gadolinium removal from contaminated aquatic systems. *Sci. Total Environ.* 749, 141488. <https://doi.org/10.1016/j.scitotenv.2020.141488>.
- Gonzalez, V., Vignati, D.A.L., Leyval, C., Giamberini, L., 2014. Environmental fate and ecotoxicity of lanthanides: are they a uniform group beyond chemistry? *Environ. Int.* 71, 148–157. <https://doi.org/10.1016/j.envint.2014.06.019>.
- Grimm, H., Williams, Sh., 2018. Gadolinium clearance times for 135 contrast MRI cases including urine test results by agent administered for 63 unconfounded cases. <https://gadoliniumtoxicity.com/gadolinium-clearance-times-for-135-contrast-mri-cases-final-v1-1/>.
- Hatje, V., Bruland, K.W., Flegal, A.R., 2016. Increases in anthropogenic gadolinium anomalies and rare earth element concentrations in San Francisco Bay over a 20 year record. *Environ. Sci. Technol.* 50, 4159–4168. <https://doi.org/10.1021/acs.est.5b04322>.
- Hatje, V., Pedreira, R.M.A., Pahnke, K., Philipp, B., 2018. Tracking hospital effluent-derived gadolinium in Atlantic coastal waters off Brazil. *Water Res.* 145, 62–72. <https://doi.org/10.1016/j.watres.2018.08.005>.
- Hayes-Labrado, L., Schillebeeckx, S.J.D., Workman, M., Shah, N., 2013. Contrasting perspectives on China's rare earths policies: reframing the debate through a stakeholder lens. *Energy Policy* 63, 55–68. <https://doi.org/10.1016/j.enpol.2013.07.121>.
- Henriques, B., Coppola, F., Monteiro, R., Pinto, J., Viana, T., Pretti, C., Soares, A., Freitas, R., Pereira, E., 2019. Toxicological assessment of anthropogenic gadolinium in seawater: biochemical effects in mussels *Mytilus galloprovincialis*. *Sci. Total Environ.* 664, 626–634. <https://doi.org/10.1016/j.scitotenv.2019.01.341>.
- Holzbecher, E., Knappe, A., Pekdeger, A., 2005. Identification of degradation characteristics exemplified by Gd-DTPA in a large experimental column. *Environ. Model. Assess.* 10, 1–8.
- Kartamihardja, A.A.P., Kumasaka, S., Hilfi, L., Kameo, S., Koyama, H., Tsumura, Y., 2022. Biosorption of different gadolinium (Gd) complexes from water by *Eichhornia crassipes* (water hyacinth). *Int. J. Phytorem.* 24, 893–901. <https://doi.org/10.1080/15226514.2021.1984388>.
- Kulaksız, S., Bau, M., 2007. Contrasting behaviour of anthropogenic gadolinium and natural rare earth elements in estuaries and the gadolinium input into the North Sea. *Earth Planet. Sci. Lett.* 260, 361–371. <https://doi.org/10.1016/j.epsl.2007.06.016>.
- Kulaksız, S., Bau, M., 2011. Anthropogenic gadolinium as a microcontaminant in tap water used as drinking water in urban areas and megacities. *Appl. Geochem.* 26, 1877–1885. <https://doi.org/10.1016/j.apgeochem.2011.06.011>.
- Künemeyer, J., Terborg, L., Meermann, B., Brauckmann, C., Möller, I., Scheffer, A., Karst, U., 2009. Speciation analysis of gadolinium chelates in hospital effluents and wastewater treatment plant sewage by a novel HILIC/ICP-MS method. *Environ. Sci. Technol.* 43 (8), 2884–2890. <https://doi.org/10.1021/es803278n>.
- Lawrence, M.G., Ort, C., Keller, J., 2009. Detection of anthropogenic gadolinium in treated wastewater in South East Queensland, Australia. *Water Res.* 43, 3534–3540. <https://doi.org/10.1016/j.watres.2009.04.033>.
- Lohrke, J., Frenzel, T., Endrikat, J., Alves, F.C., Grist, T.M., Law, M., Lee, J.M., Leiner, T., Li, K.C., Nikolaou, K., Prince, M.R., Schild, H.H., Weinreb, J.C., Yoshikawa, K., Pietsch, H., 2016. 25 years of contrast-enhanced MRI: developments, current challenges and future perspectives. *Adv. Ther.* 33, 1–28. <https://doi.org/10.1007/s12325-015-0275-4>.
- McDonald, R.J., Levine, D., Weinreb, J., Kanal, E., Davenport, M.S., Ellis, J.H., Jacobs, P.M., Lenkinski, R.E., Maravilla, K.R., Prince, M.R., Rowley, H.A., Tweedie, M.F., Kressel, H.Y., 2018. Gadolinium retention: a research roadmap from the 2018 NIH/ACR/RSNA workshop on gadolinium chelates. *Radiology* 289, 517–534. <https://doi.org/10.1148/radiol.2018181151>.
- Möller, P., Paces, T., Dulski, P., Morteani, G., 2002. Anthropogenic gd in surface water, drainage system, and the water supply of the city of Prague, Czech Republic. *Environ. Sci. Technol.* 36, 2387–2394. <https://doi.org/10.1021/ES010235Q>.
- Nance, W.B., Taylor, S.R., 1976. Rare earth element patterns and crustal evolution-I. Australian post-archean sedimentary rocks. *Geochim. Cosmochim. Acta* 40, 1539–1551. [https://doi.org/10.1016/0016-7037\(76\)90093-4](https://doi.org/10.1016/0016-7037(76)90093-4).
- Qizhong, W., Suhua, Y., Fuging, S., Yugi, W., Bingru, C., Shude, T., Jingxin, S., 1985. Rare-earth elements in luochuan loess section, Shaanxi province. *Geochemistry* 4, 172–180. <https://doi.org/10.1007/BF03179337>.
- Rabiet, M., Brissaud, F., Seidel, J.L., Pistre, S., Elbaz-Poulichet, F., 2009. Positive gadolinium anomalies in wastewater treatment plant effluents and aquatic environment in the Hérault watershed (South France). *Chemosphere* 75, 1057–1064. <https://doi.org/10.1016/j.chemosphere.2009.01.036>.
- Schmidt, K., Bau, M., Merschel, G., Tepe, N., 2019. Anthropogenic gadolinium in tap water and in tap water-based beverages from fast-food franchises in six major cities in Germany. *Sci. Total Environ.* 687, 1401–1408. <https://doi.org/10.1016/j.scitotenv.2019.07.075>.
- Souza, L.A., Pedreira, R.M.A., Miró, M., Hatje, V., 2021. Evidence of high bioaccessibility of gadolinium-contrast agents in natural waters after human oral uptake. *Sci. Total Environ.* 793, 148506. <https://doi.org/10.1016/j.scitotenv.2021.148506>.
- Swan, S.K., Lambrecht, L.J., Townsend, R., Davies, B.E., McCloud, S., Parker, J.R., Bensch, K., LaFrance, N.D., 1999. Safety and pharmacokinetic profile of gadobenate dimeglumine in subjects with renal impairment. *Investig. Radiol.* 34, 443–448.
- Telgmann, L., Wehe, C.A., Birka, M., Künemeyer, J., Nowak, S., Sperling, M., Karst, U., 2012. Speciation and isotope dilution analysis of gadolinium-based contrast agents in wastewater. *Environ. Sci. Technol.* 46, 11929–11936. <https://doi.org/10.1021/es301981z>.
- Tircsó, G., Molnár, E., Csupász, T., Garda, Z., Botár, R., Kálmán, F.K., Kovács, Z., Brücher, E., Tóth, I., 2021. 2 Gadolinium(III)-based contrast agents for magnetic resonance imaging. A re-appraisal. In: Sigel, A., Freisinger, E., Sigel, R.K.O. (Eds.), *Metal Ions in Bio-imaging Techniques*. 2021. De Gruyter. <https://doi.org/10.1515/9783110685701-008>.
- Verplanck, P., Taylor, H.E., Nordstrom, D.K., Barber, L.B., 2005. Aqueous stability of gadolinium in surface waters receiving sewage treatment plant effluent, Boulder Creek, Colorado. *Environ. Sci. Technol.* 39, 6923–6929. <https://doi.org/10.1021/ES048456U>.

- Verplanck, P., Furlong, E.T., Gray, J.L., Philips, P.J., Wolf, R.E., Esposito, K., 2010. Evaluating the behavior of gadolinium and other rare earth elements through large metropolitan sewage treatment plants. *Environ. Sci. Technol.* 44, 3876–3882.
- Wahsner, J., Gale, E.M., Rodríguez-Rodríguez, A., Caravan, P., 2019. Chemistry of MRI contrast agents: current challenges and new frontiers. *Chem. Rev.* 119, 957–1057. <https://doi.org/10.1021/acs.chemrev.8b00363>.
- Zeng, Y.H., Huai, W.X., 2014. Estimation of longitudinal dispersion coefficient in rivers. *J. Hydro Environ. Res.* 8, 2–8. <https://doi.org/10.1016/j.jher.2013.02.005>.
- Zhu, Y., Hoshino, M., Yamada, H., Itoh, A., Haraguchi, H., 2004. Gadolinium anomaly in the distributions of rare earth elements observed for coastal seawater and river waters around Nagoya City. *Bull. Chem. Soc. Jpn.* 77, 1835–1842. <https://doi.org/10.1246/bcsj.77.1835>.
- Zocher, A.L., Klimpel, F., Kraemer, D., Bau, M., 2022. Naturally grown duckweeds as quasi-hyperaccumulators of rare earth elements and yttrium in aquatic systems and the bioavailability of gadolinium-based MRI contrast agents. *Sci. Tot. Env.* 838 (Part 2), 155909. <https://doi.org/10.1016/j.scitotenv.2022.155909>.